

Tunable Corrosion Behavior of Calcium Phosphate Coated Fe-Mn-Si Alloys for Bone Implant Applications



RICHARD DREVET, YULIA ZHUKOVA, PULAT KADIROV, SERGEY DUBINSKIY, ALIBEK KAZAKBIEV, YURY PUSTOV, and SERGEY PROKOSHKIN

This work deals with the electrodeposition of calcium phosphate coatings on the surface of Fe-Mn-Si alloys which is designed for bone implant applications. Three different alloy compositions are considered (Fe-23Mn-5Si, Fe-26Mn-5Si and Fe-30Mn-5Si, all in wt pct). In order to explore the impact of hydrogen peroxide (H_2O_2) on the electrodeposition process, two different electrolytic solutions are studied, one that contains no H_2O_2 and the other that contains 9 vol pct H_2O_2 . The physicochemical characterizations reveal that the electrodeposited coating is made of an apatite phase of low crystallinity with less porosity when hydrogen peroxide is added to the electrolyte solution. The corrosion measurements of the uncoated and coated alloys are also carried out during immersion in Hank's solution at 310 K (37 °C), a physiological solution that simulates the inorganic composition of the body fluids. Interestingly, it was found that the manganese content in the alloy and the porosity of the coating both modify the corrosion behavior, *i.e.*, the biodegradability of the Fe-Mn-Si alloy immersed in the physiological environment. Hence, the corrosion behavior of the calcium phosphate-coated Fe-Mn-Si alloys is tunable as a function of the experimental parameters used during the synthesis of the material.

<https://doi.org/10.1007/s11661-018-4907-6>

© The Minerals, Metals & Materials Society and ASM International 2018

I. INTRODUCTION

IN recent years, the biodegradable alloys have been extensively developed in the biomedical field with the purpose to be used as temporary bone implants.^[1,2] Their biodegradation properties in a natural corrosive environment such as the human body are used to bypass additional surgical intervention for the implant removal after the completion of the healing process.^[3-6] Among the biodegradable metallic materials, the Fe-Mn-Si alloys are the most promising ones due to their appropriate biomechanical compatibility and mechanical reliability with the bone tissues.^[7,8] Moreover, they degrade inside the human body faster than pure iron which is known to have relatively lower degradation rate of 0.1 mm year⁻¹^[8,9] when compared with the magnesium alloys processing with high degradation rates of 2.0 mm year⁻¹.^[10,11] Additionally, it is also noteworthy

that iron, manganese, and silicon are non-toxic elements for the human body since they are well established to be essential for the body function of all mammals.^[3,6] To date, previous studies have shown that the Fe-Mn-Si alloys with manganese contents between 23 and 30 wt pct have the most appropriate biomechanical compatibility with the bone tissues.^[8,12,13] Moreover, this range of composition is the most suitable one for microstructural, magnetic, and toxicological considerations.^[14,15] To support the bone growth during the healing process, the surface of the Fe-Mn-Si alloys can be coated with bioactive materials such as calcium phosphate ceramics whose chemical composition is similar to the mineral phase of the surrounding bone tissues.^[16-18] Several methods can be used to synthesize calcium phosphate coatings onto implant surfaces, *e.g.*, plasma spraying,^[19] sol-gel,^[20] pulsed laser-deposition,^[21] electrophoretic deposition,^[22] or electrodeposition.^[23] Among these processes, electrodeposition is the most attractive one considering low temperatures involved and a possibility to control the thickness and the chemical composition of the synthesized coatings. The electrodeposition of calcium phosphate coatings has been extensively developed for titanium alloys implants, but very few research works have considered this process for Fe-Mn-Si alloys.^[24] However, owing to

RICHARD DREVET, YULIA ZHUKOVA, PULAT KADIROV, SERGEY DUBINSKIY, ALIBEK KAZAKBIEV, YURY PUSTOV, and SERGEY PROKOSHKIN are with National University of Science and Technology "MISIS", Leninskiy prosp. 4, Moscow 119049, Russian Federation. Contact e-mail: richarddrevet@misis.ru

Manuscript submitted April 20, 2018.

Article published online September 28, 2018

insulating characteristics, the bioceramic coating can sufficiently impact the corrosion behavior, *i.e.*, the biodegradability of the Fe-Mn-Si implant material in a physiological environment. This study investigates the impact of electrodeposited calcium phosphate coatings on the corrosion behavior of Fe-Mn-Si alloys immersed in Hank's solution at 310 K (37 °C), a physiological solution that simulates the inorganic composition of the body fluids.

II. MATERIALS AND METHODS

A. Synthesis of the Fe-Mn-Si Alloys

In the present study, Fe-23Mn-5Si, Fe-26Mn-5Si, and Fe-30Mn-5Si (all the compositions are hereinafter described in weight percent) alloys ingots were prepared while using arc remelting process with a non-consumable tungsten electrode. The standard raw materials used to synthesize the aforementioned compositions were *Armco* commercially pure iron (99.85 pct), manganese (99 pct), and silicon (99 pct). After the melting process, the ingots were annealed in an electrical furnace at 1173 K (900 °C) for 60 minutes in air and then were water-quenched. The oxide layer formed on the Fe-Mn-Si alloys during the annealing treatment was removed mechanically from the surface of the ingots while using coarse grained emery paper. According to our recent work, this protocol results in homogeneous Fe-Mn-Si alloys ingots with a low impurity level.^[8] At last, 1-mm-thick sections of the three ingots were cut with a cut-off machine (*ATM Brillant 220*). The obtained samples were cleaned for 1 minute while of immersion in nitric acid (HNO₃, 10 vol pct) followed by 1 minute of ultrasonic cleaning in isopropanol.

B. Synthesis of the Calcium Phosphate Coating

The calcium phosphate coatings electrodepositions were carried out with a classical three-electrode system. The cathode was the Fe-Mn-Si alloy whose dimensions were 10 mm × 10 mm × 1 mm. The counter electrode was a gold plate and the reference electrode was a saturated silver chloride electrode (SSCE). The three electrodes were immersed in the electrolytic solution at 333 K (60 °C) prepared by dissolving 0.042 M Ca(NO₃)₂·4H₂O and 0.025 M NH₄(H₂PO₄) in deionized water. According to our previous protocols, the experiments were conducted first with no hydrogen peroxide in the electrolyte solution (0 vol pct H₂O₂) and then with hydrogen peroxide (9 vol pct H₂O₂), with the highest amount usable for the process.^[25] The electrodeposition was carried out with an IPC-Pro electronic potentiostat (*Volta Co*) by pulsing the current during five cycles. Each cycle was composed by a deposition time of 1 minute with a current density of -15 mA cm^{-2} following by a break time of 2 minutes at 0 mA cm⁻² as explicitly indicated in Figure 1.

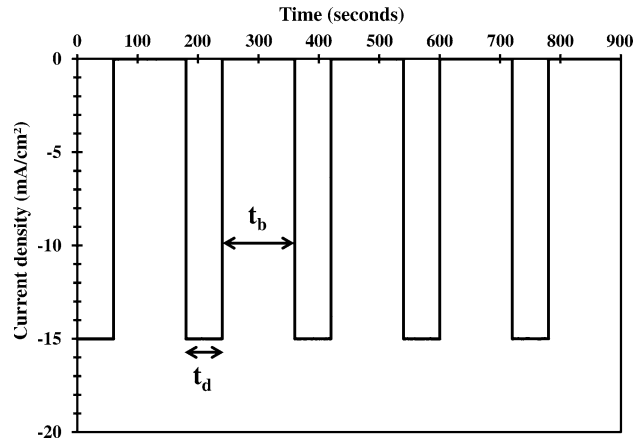


Fig. 1—Pulsed current applied for the electrodeposition of the calcium phosphate coatings. Five cycles of deposition time ($t_d = 1 \text{ min}$) and break time ($t_b = 2 \text{ min}$).

C. Physicochemical Characterization of the Calcium Phosphate-Coated Fe-Mn-Si Alloys

The coatings morphology was observed with a LaB₆ scanning electron microscope (SEM, *JEOL JSM-6480LV*) equipped with an energy-dispersive spectrometer (EDS, *JED-2300F*). The characteristic Ca/P atomic ratio of the coatings was determined by X-ray microanalysis obtained from the acquired EDS spectra. In order to get a representative value of these quantifications, three EDS spots were acquired in different zones of the coating. The presented values corresponded to the average of these triplicate measurements. The phase composition of the electrodeposited coatings was studied by X-ray diffraction (XRD) with a *DRON-3* diffractometer using a Cu K α radiation. The phases were identified from the diffraction files provided by the International Centre for Diffraction Data (ICDD).

D. Electrochemical Study in Physiological Solution

The potentiodynamic polarization experiments were used to assess the corrosion properties of the calcium phosphate-coated Fe-Mn-Si alloys. These electrochemical characterizations were carried out in Hank's solution at 310 K (37 °C) that mimics the chemical composition of the body fluids according to the concentrations of the salts dissolved in 1 L of distilled water: 8 g NaCl, 0.4 g KCl, 0.12 g Na₂HPO₄·12H₂O, 0.06 g KH₂PO₄, 0.2 g MgSO₄·7H₂O, 0.35 g NaHCO₃, and 0.14 g CaCl₂ (pH 7.4). The polarization of the samples was applied with an IPC-Pro electronic potentiostat (*Volta Co*). The reference electrode was a SSCE, and the counter electrode was a gold electrode. The polarization diagrams were recorded with a scan rate of 1.0 mV s⁻¹. All the measurements were performed in triplicate. From the Tafel representation of the polarization curves, the corrosion current density (i_{corr}) was extracted to determine the corrosion rate (C_r) of the alloys as follows^[8]:

$$C_r = \frac{i_{\text{corr.}} \times A \times 10^4}{n \times F \times \rho}, \quad [1]$$

where A was the atomic mass of the alloy; n was the number of the transferred electrons according to the corrosion reaction, and F was the Faraday constant ($F = 96,500 \text{ C mol}^{-1}$).

III. RESULTS AND DISCUSSION

A. Synthesis and Characterizations of the Calcium Phosphate Coatings Electrodeposited on the Fe-Mn-Si Alloys

The electrodeposition of the calcium phosphate coatings is successfully carried out on the surface of the Fe-Mn-Si alloys according to the pulsed current mode displayed in Figure 1. The corresponding potential variations are presented in Figures 2(a) and (b) for the coatings synthesized from the 0 vol pct H_2O_2 solution and from the 9 vol pct H_2O_2 solution, respectively.

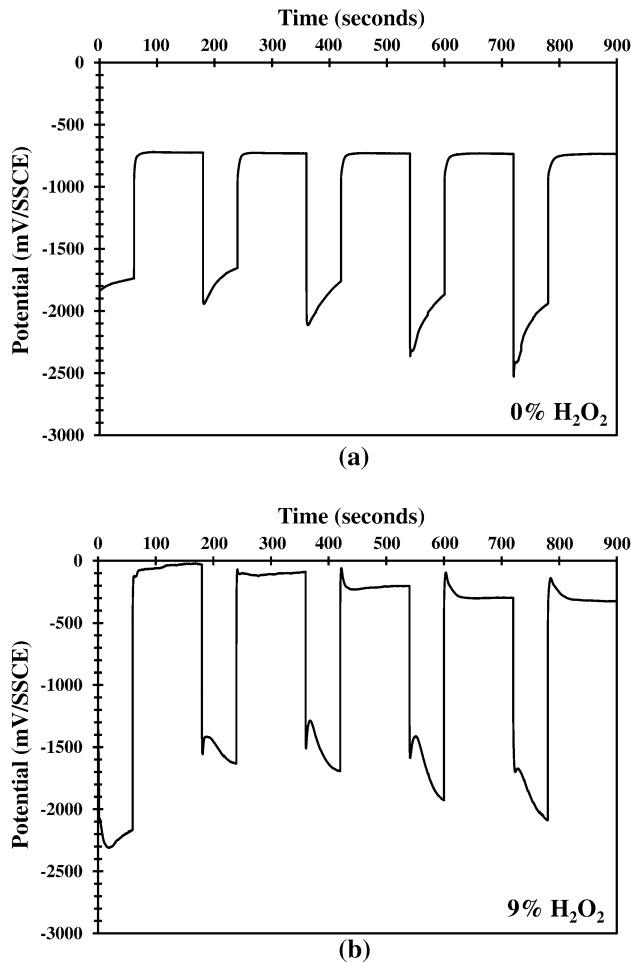
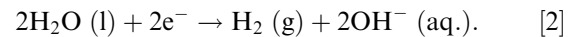


Fig. 2—Chronopotentiometric curves during pulsed electrodeposition (a) in the 0 vol pct H_2O_2 solution and (b) in the 9 vol pct H_2O_2 solution.

According to the electrolyte composition, the chronopotentiometric curves exhibit different potential evolutions during the five-pulsed current cycles. In case of the experiments carried out from the 0 vol pct H_2O_2 solution (Figure 2(a)), the increasing potential during each minute of deposition indicates that the metallic surface is progressively modified by the growth of the calcium phosphate coating. The more the calcium phosphate coating is deposited, the more the potential varies. During the break times, the surface of the sample reaches a constant free potential value during which the electrolyte solution is homogenized recovering its initial state.^[26] In case of the experiments carried out from the 9 vol pct H_2O_2 solution (Figure 2(b)), the whole potential values are shifted towards more positive values. During the deposition times, the potential varies in two steps: first, increasing and then decreasing continually until the break time. The difference between these two electrochemical behaviors is linked to the electrolyte compositions. In the 0 vol pct H_2O_2 solution, the reduction of water is the only electrochemical reaction occurring at the cathode during the deposition process according to reaction [2]:



This reduction reaction produces a local modification of the pH value in the vicinity of the Fe-Mn-Si alloy, inducing the precipitation of the calcium phosphate coating.^[27] Kuo *et al.* have shown that the reaction [2] promotes the presence of H_2 bubbles at the cathode that produces craters and holes inside the coating.^[28] Therefore, only low current densities can be used with a direct current mode ($j_{\text{max}} = 10 \text{ mA cm}^{-2}$) resulting on low basic pH values at the cathode ($\text{pH}_{\text{max}} 8$).^[29] The range of chemical compositions reachable for the calcium phosphate coating is then limited. For example, Zhang *et al.* have obtained layers made of a mixture of brushite and octacalcium phosphate with a current density of 3 mA cm^{-2} .^[30] Abdel-Aal *et al.* have obtained brushite layers with current densities up to 6 mA cm^{-2} .^[31] At last, Dumelié *et al.* have synthesized coatings made of octacalcium phosphate mixed with a calcium-deficient apatitic phase by applying a current density of 10 mA cm^{-2} .^[32] In contrast, with a pulsed current mode, current densities up to 15 mA cm^{-2} can be used increasing the range of the possible chemical compositions for the electrodeposited coating.^[27] More chemical compositions are accessible by addition of hydrogen peroxide (H_2O_2) to the electrolyte solution. In the 9 vol pct H_2O_2 solution, the reduction of water occurs simultaneously with the reduction of hydrogen peroxide according to reaction [3]:



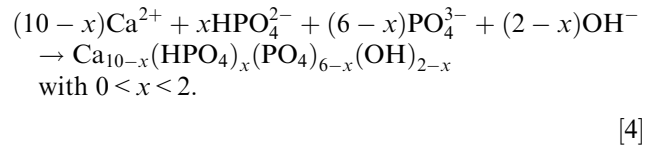
I. Zhitomirsky explains that the addition of H_2O_2 is limited to 9 vol pct because “when the rate of OH^- generation is faster than the rate of OH^- consumption by hydrolysis reactions at the electrode, a fraction of the OH^- ions generated at the cathode is transported away

by the electric current and the diffusion. In this case, the high pH boundary moves away from the electrode surface, resulting in lower adhesion of the deposits.^[33]

Several studies have described the impact of these electrochemical reactions on the deposition of the calcium phosphate coating that occurs in two steps, *i.e.*, an instantaneous nucleation followed by a progressive three-dimensional growth.^[29,34] Hydrogen peroxide modifies the calcium phosphate crystals growth and impacts the morphology of the obtained coating.^[25] The SEM images of Figure 3 show the morphology of the coatings electrodeposited in both conditions.

The coating electrodeposited from the 0 vol pct H₂O₂ solution (Figure 3(a)) is made of more porosity in comparison with the coating electrodeposited from the 9 vol pct H₂O₂ solution (Figure 3(b)). Indeed, hydrogen peroxide is a strong oxidative reagent, preferentially reduced at the cathode during the electrodeposition process. The corresponding reduction reaction produces only hydroxide ions (OH⁻) without any dihydrogen (H₂) bubbles, according to reaction [3]. The corresponding increase of the pH value promotes the precipitation of calcium phosphate coatings with less porosity than the coatings electrodeposited from the solution in which water is the only solvent. The chemical and the structural characterizations of the calcium phosphate coated Fe-Mn-Si alloys are presented in the EDS spectra of Figure 4 and the XRD profiles of Figure 5, respectively.

Under any experimental conditions attributed for the electrodeposition process, the formation of the coating is characterized by a stoichiometric apatite phase of low crystallinity. The characteristic Ca/P atomic ratio is 1.43 for the coating electrodeposited from the 0 vol pct H₂O₂ solution and 1.54 for the coating electrodeposited from the 9 vol pct H₂O₂ solution. Moreover, it is noticeable that no impurity is detected from the EDS analyses and no other phases than apatite on the substrate from XRD. These results point out that the electrodeposition process produces calcium-deficient apatite coatings precipitated according to reaction [4]:



Nevertheless, these results show that the pulsed current electrodeposition process previously developed for titanium alloys can be transposed to coat Fe-Mn-Si alloys.^[25,27] The obtained calcium phosphate coatings are chemically and structurally similar to those electrodeposited on titanium alloys. These coatings improve the bioactivity of the implant material, promoting the proliferation of the MG-63 cells without any cytotoxic effect. Moreover, they induce an overexpression of the main gene markers involved in the bone formation.^[35]

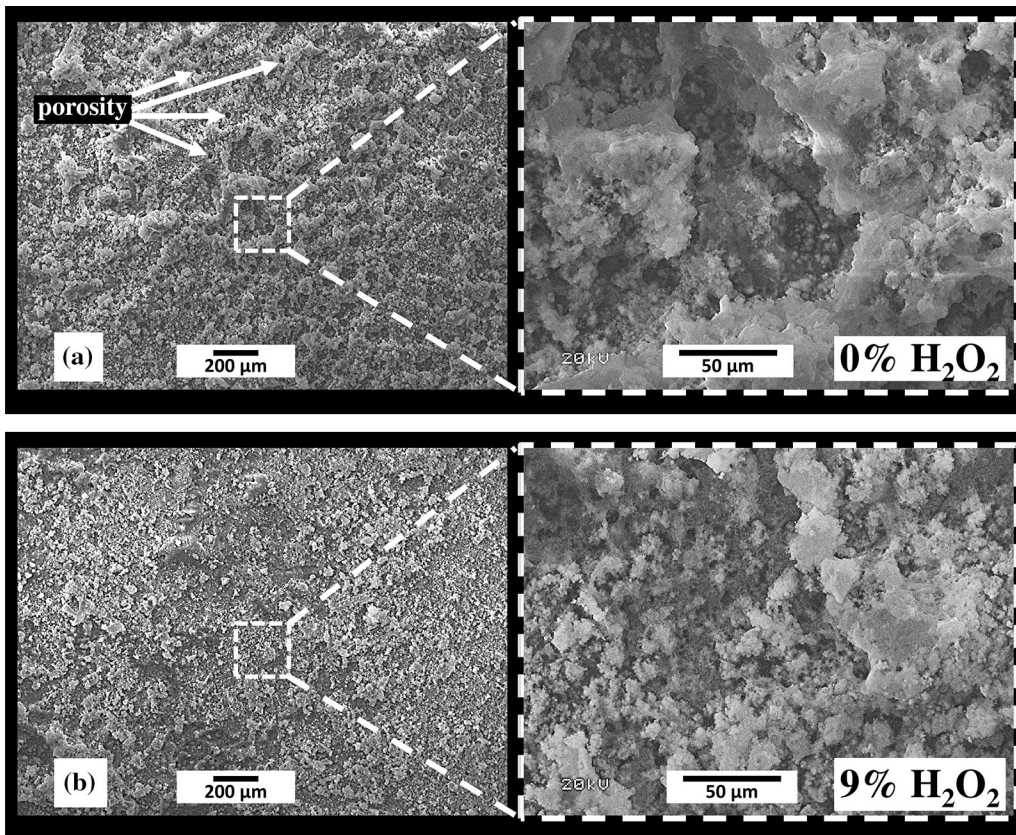


Fig. 3—SEM images of the calcium phosphate coating electrodeposited (a) from the 0 vol pct H₂O₂ solution and (b) from the 9 vol pct H₂O₂ solution.

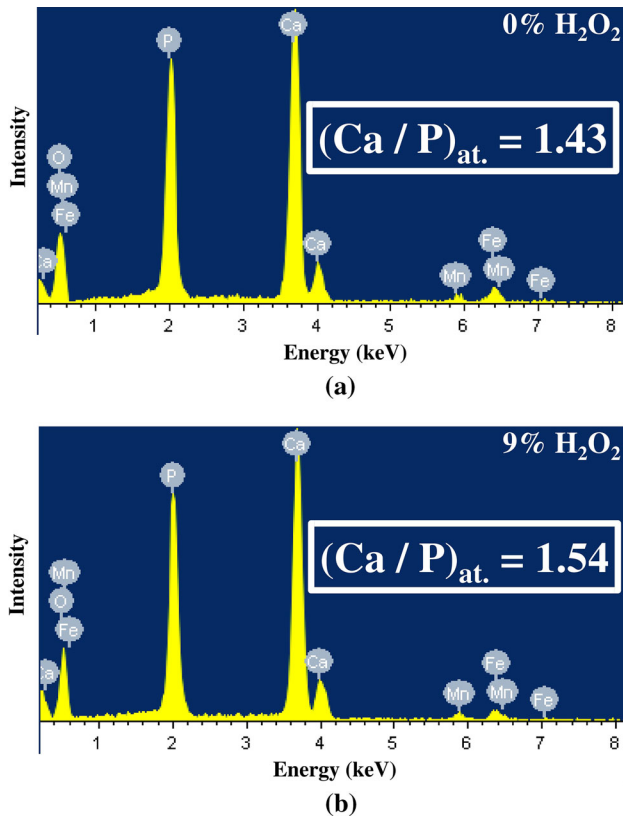


Fig. 4—EDS spectra of the calcium phosphate coated Fe-Mn-Si alloy from the 0 vol pct H_2O_2 solution and (b) from the 9 vol pct H_2O_2 solution.

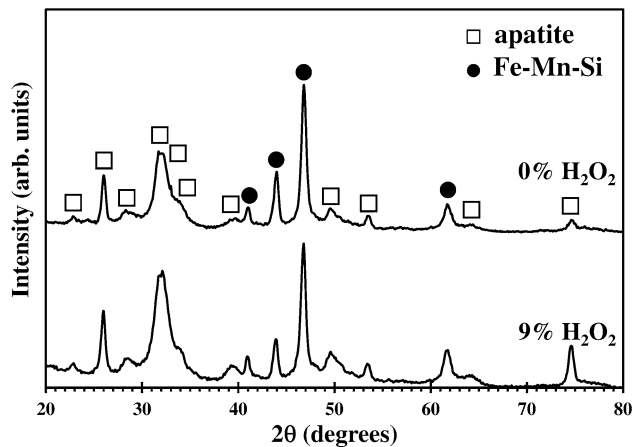


Fig. 5—XRD patterns of the calcium phosphate coated Fe-Mn-Si alloy from the 0 vol pct H_2O_2 solution and from the 9 vol pct H_2O_2 solution.

However, the present study concerns Fe-Mn-Si alloys with a perspective to use them as biodegradable bone implants. Therefore, the impact of the produced coatings on the corrosion behavior of the alloys has to be assessed in physiological solution.

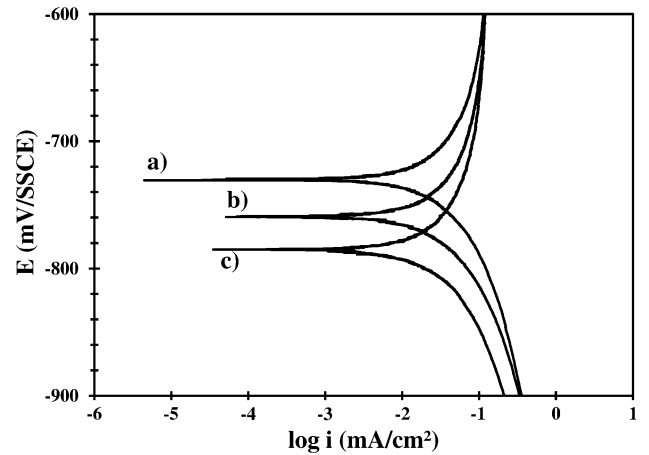


Fig. 6—Polarization diagrams in Hank's solution at 310 K (37 °C) of (a) Fe-23Mn-5Si, (b) Fe-26Mn-5Si, and (c) Fe-30Mn-5Si.

B. Corrosion Behavior in Physiological Solution of the Calcium Phosphate-Coated Fe-Mn-Si Alloys

The polarization measurements carried out during immersions tests in Hank's solution at 310 K (37 °C) are displayed in Figures 6 and 7. They highlight the impact of the manganese content on the corrosion behavior of the Fe-Mn-Si alloys (Figure 6) and the impact of the electrodeposited calcium phosphate coatings on their surfaces (Figure 7).

The polarization diagrams of the three uncoated alloys (Fe-23Mn-5Si, Fe-26Mn-5Si, and Fe-30Mn-5Si) are presented and compared to those obtained with the coatings electrodeposited from the 0 vol pct H_2O_2 solution and from the 9 vol pct H_2O_2 solution. The corresponding corrosion potentials (E_{corr}) and the corrosion current densities (i_{corr}) extracted from these curves are gathered in Tables I and II, respectively.

The comparison of the three uncoated alloys indicates that the manganese amount in the Fe-Mn-Si system modifies the corrosion behavior of the implant material. When the manganese amount increases from 23 to 26 and 30 wt pct, the corrosion potential of the Fe-Mn-Si alloy is shifted towards more negative values (Table I).

This observation points out an increase in the corrosion behavior of the alloy from a thermodynamic point of view. Nonetheless, manganese has a more negative standard potential than iron that promotes the electrochemical activity in the physiological solution.^[36,37] Similarly, the corrosion behavior of the alloy is also modified from a kinetics point of view, as described by an increase of corrosion current density, *i.e.*, the corrosion rate, with the manganese content (Tables II and III).

In contrary, the electrodeposition of a calcium phosphate coating on the surface of the Fe-Mn-Si alloys decreases the corrosion rate of the implant material. In that case, the corrosion potential of the material is shifted towards more positive values and,

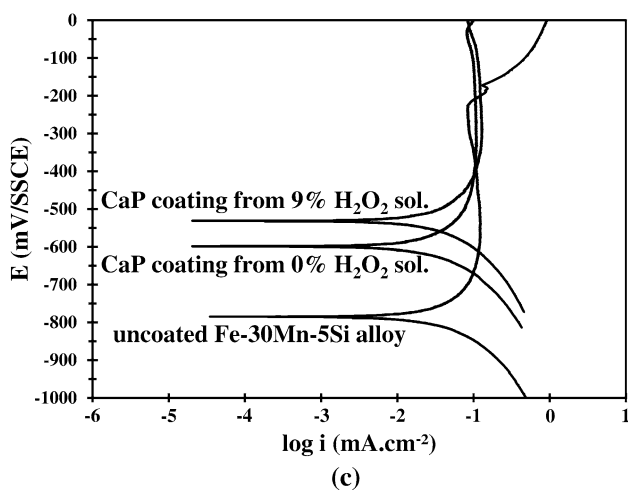
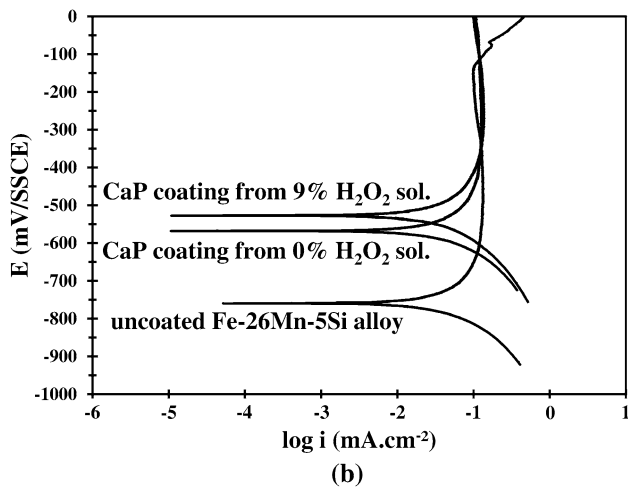
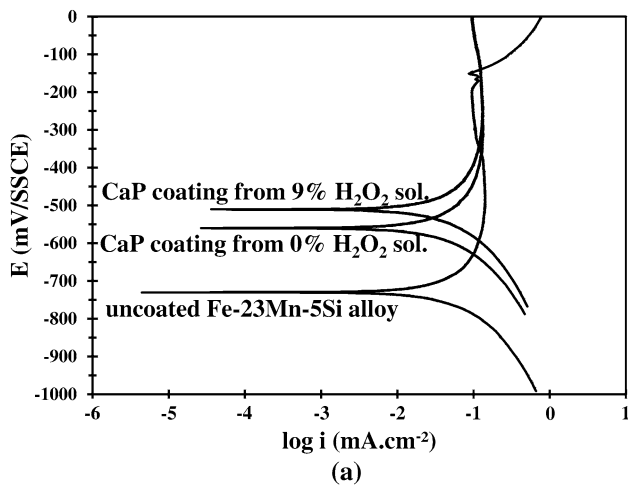


Fig. 7—Polarization diagrams in Hank's solution at 310 K (37 °C) of the uncoated and the calcium phosphate-coated Fe-Mn-Si alloys from the 0 vol pct H_2O_2 solution and from the 9 vol pct H_2O_2 solution: case of (a) Fe23Mn5Si, (b) Fe26Mn5Si, and (c) Fe30Mn5Si.

simultaneously, the corrosion current density decreases. Particularly, these variations are more pronounced with the coatings electrodeposited from the 9 vol pct H_2O_2

solution in comparison with those electrodeposited from the 0 vol pct H_2O_2 solution.

These results show that the electrodeposited coatings act as insulating barriers for the Fe-Mn-Si alloys, thereby mitigating the corrosion reactions induced by the aggressive physiological solution. This is reasonable considering the fact that the immersion of metallic implants in a physiological solution induces ionic attacks of the alloy by electrochemical reactions at the solid-liquid interface.^[38] Since the calcium phosphate coatings are ceramic materials, they partially insulate the metallic surface from the solution and reduce the impact of the corrosion reactions at the interface.^[39] Nevertheless, the electrodeposited coatings are porous and the electrolyte is able to fill the pores reaching the metallic surface to produce the corrosion reactions. As a function of the electrolyte solution used, the morphology and the topography of the calcium phosphate coating are modified, effecting the corrosion behavior of the implant. As previously explained, the calcium phosphate coating electrodeposited from the 9 vol pct H_2O_2 solution is less porous because the reduction of H_2O_2 (reaction [3]) does not produce H_2 bubbles during the deposition unlike the reduction of water (reaction [2]). Therefore, the penetration of the physiological solution through the coating is lessened, and the surface of the Fe-Mn-Si alloy is more insulated with the coatings electrodeposited from the 9 vol pct H_2O_2 solution.

Consequently, the corrosion behavior of the calcium phosphate-coated Fe-Mn-Si alloy can be tuned on one hand by adjusting the manganese content of the alloy (from 23 to 30 wt pct) and on the other hand by the concentration of hydrogen peroxide in the electrolyte solution (from 0 to 9 vol pct). These two experimental parameters are sufficiently well correlated during the synthesis process to produce the bone implant material with the most optimum corrosion behavior for a targeted application.

IV. CONCLUSIONS

In this work, calcium phosphate coatings have been electrodeposited on the surface of Fe-Mn-Si alloys used for bone implant applications. The polarization measurements have shown that the manganese amount in the alloy impacts the corrosion behavior of the alloy due to a more negative standard potential of manganese in comparison with that of iron. Therefore, the electrochemical activity of the alloy increases with the manganese amount in the alloy. On the other hand, the corrosion rate of the alloy is reduced by the insulating properties of the electrodeposited calcium phosphate coating. When hydrogen peroxide is added to the electrolyte solution used to synthesize it, the calcium phosphate coating is less porous and the insulation of Fe-Mn-Si alloys increases. Consequently, these two experimental parameters are powerful tools to produce new implant materials with the most appropriate corrosion behavior, *i.e.*, with a chosen biodegradability inside the body.

Table I. Corrosion Potentials of the Uncoated and the Calcium Phosphate Coated Fe-Mn-Si Alloys

	Corrosion Potential, E_{corr} (mV/SSCE)		
	Fe-23Mn-5Si	Fe-26Mn-5Si	Fe-30Mn-5Si
CaP Coating from 9 Pct H ₂ O ₂ Sol.	- 510 ± 11	- 528 ± 11	- 531 ± 11
CaP Coating from 0 Pct H ₂ O ₂ Sol.	- 560 ± 12	- 568 ± 12	- 599 ± 12
Uncoated Fe-Mn-Si Alloys	- 730 ± 15	- 753 ± 16	- 785 ± 16

Table II. Corrosion Current Density of the Uncoated and the Calcium Phosphate Coated Fe-Mn-Si Alloys

	Corrosion Current Density, i_{corr} ($\mu\text{A cm}^{-2}$)		
	Fe-23Mn-5Si	Fe-26Mn-5Si	Fe-30Mn-5Si
CaP Coating from 9 Pct H ₂ O ₂ Sol.	18 ± 1	21 ± 1	27 ± 2
CaP Coating from 0 Pct H ₂ O ₂ Sol.	29 ± 2	38 ± 2	42 ± 3
Uncoated Fe-Mn-Si Alloys	46 ± 3	55 ± 3	70 ± 4

Table III. Corrosion Rate (C_r) of the Uncoated and the Calcium Phosphate Coated Fe-Mn-Si Alloys

	Corrosion Rate, C_r (mm year ⁻¹)		
	Fe-23Mn-5Si	Fe-26Mn-5Si	Fe-30Mn-5Si
CaP Coating from 9 Pct H ₂ O ₂ Sol.	0.21 ± 0.01	0.25 ± 0.01	0.32 ± 0.02
CaP Coating from 0 Pct H ₂ O ₂ Sol.	0.35 ± 0.02	0.45 ± 0.02	0.50 ± 0.04
Uncoated Fe-Mn-Si Alloys	0.54 ± 0.04	0.65 ± 0.04	0.84 ± 0.05

ACKNOWLEDGMENTS

The present work was carried out with the financial support of the Ministry of Education and Science of the Russian Federation, in the framework of the Increase Competitiveness Program of NUST "MISIS" (Grant No. K4-2016-57). The authors thank Dr. E. Bazanova, NUST "MISIS" Director of Academic Writing Office, and Dr. M.F. Ijaz for their critical reading of the manuscript and some helpful suggestions.

REFERENCES

1. Y.F. Zheng, X.N. Gu, and F. Witte: *Mater. Sci. Eng. R*, 2014, vol. 77, pp. 1–34.
2. H. Li, Y. Zheng, and L. Qin: *Prog. Nat. Sci.*, 2014, vol. 24, pp. 414–22.
3. M. Niinomi: *Metall. Mater. Trans. A*, 2002, vol. 33A, pp. 477–86.
4. H. Hermawan, D. Dubé, and D. Mantovani: *Acta Biomater.*, 2010, vol. 6, pp. 1693–97.
5. M. Schinhammer, A.C. Hänni, J.F. Löffler, and P.J. Uggowitzer: *Acta Biomater.*, 2010, vol. 6, pp. 1705–13.
6. A. Francis, Y. Yang, S. Virtanen, and A.R. Boccaccini: *J. Mater. Sci.*, 2015, vol. 26, pp. 138–53.
7. C.H. Yang, H.C. Lin, K.M. Lin, and H.K. Tsai: *Mater. Sci. Eng. A*, 2008, vol. 497, pp. 445–50.
8. R. Drevet, Y. Zhukova, P. Malikova, S. Dubinskiy, A. Korotitskiy, Y. Pustov, and S. Prokoshkin: *Metall. Mater. Trans. A*, 2018, vol. 49A, pp. 1006–13.
9. T. Niendorf, F. Brenne, P. Hoyer, D. Schwarze, M. Schaper, R. Grothe, M. Wiesener, G. Grundmeier, and H.J. Maier: *Metall. Mater. Trans. A*, 2015, vol. 46A, pp. 2829–33.
10. F. Witte: *Acta Biomater.*, 2010, vol. 6, pp. 1680–92.
11. Y. Chen, Z. Xu, C. Smith, and J. Sankar: *Acta Biomater.*, 2014, vol. 10, pp. 4561–73.
12. H. Hermawan, D. Dubé, and D. Mantovani: *J. Biomed. Mater. Res.*, 2010, vol. 93A, pp. 1–11.
13. M. Kaya and O. Cakmak: *Metall. Mater. Trans. A*, 2016, vol. 47A, pp. 1499–1503.
14. Y.P. Feng, N. Gaztelumendi, J. Fornell, H.Y. Zhang, P. Solsona, M.D. Baró, S. Suriñach, E. Ibáñez, L. Barrios, E. Pellicer, C. Nogués, and J. Sort: *J. Alloy Compd*, 2017, vol. 724, pp. 1046–56.
15. Y.P. Feng, A. Blanquer, J. Fornell, H. Zhang, P. Solsona, M.D. Baró, S. Suriñach, E. Ibáñez, E. García-Lecina, X. Wei, R. Li, L. Barrios, E. Pellicer, C. Nogués, and J. Sort: *J. Mater. Chem. B*, 2016, vol. 4, pp. 6402–12.
16. S.R. Paital and N.B. Dahotre: *Mater. Sci. Eng. R*, 2009, vol. 66, pp. 1–70.
17. S.V. Dorozhkin: *Mater. Sci. Eng. C*, 2015, vol. 55, pp. 272–326.
18. R.A. Surmenev, M.A. Surmeneva, and A.A. Ivanova: *Acta Biomater.*, 2014, vol. 10, pp. 557–79.
19. R.B. Heilmann: *Surf. Coat. Technol.*, 2006, vol. 201, pp. 2012–19.
20. C. Domínguez-Trujillo, E. Peón, E. Chicardi, H. Pérez, J.A. Rodríguez-Ortiz, J.J. Pavón, J. García-Couce, J.C. Galván, F. García-Moreno, and Y. Torres: *Surf. Coat. Technol.*, 2018, vol. 333, pp. 158–62.
21. R.A. Ismail, E.T. Salim, and W.K. Hamoudi: *Mater. Sci. Eng. C*, 2013, vol. 33, pp. 47–52.
22. M. Farrokhi-Rad: *Surf. Coat. Technol.*, 2017, vol. 329, pp. 155–62.
23. M. Ibrahim Coskun, I.H. Karahan, Y. Yücel, and T.D. Golden: *Surf. Coat. Technol.*, 2016, vol. 301, pp. 42–53.

24. J. Fornell, Y.P. Feng, E. Pellicer, S. Suriñach, M.D. Baró, and J. Sort: *J. Alloy Compd.*, 2017, vol. 729, pp. 231–39.
25. R. Drevet, H. Benhayoune, L. Wortham, S. Potiron, J. Douglade, and D. Laurent-Maquin: *Mater. Charact.*, 2010, vol. 61, pp. 786–95.
26. F.A. Azem, T.K. Delice, G. Ungan, and A. Cakir: *Mater. Sci. Eng. C*, 2016, vol. 68, pp. 681–86.
27. R. Drevet and H. Benhayoune: in *Calcium Phosphate: Structure, Synthesis, Properties, and Applications*, R.B. Heimann, ed., Nova Science Publishers, Inc., New York, 2012, pp. 231–52.
28. M.C. Kuo and S.K. Yen: *Mater. Sci. Eng. C*, 2002, vol. 20, pp. 153–60.
29. N. Eliaz and T.M. Sridh: *Cryst. Growth Des.*, 2008, vol. 8, pp. 3965–77.
30. J.M. Zhang, C.J. Lin, Z.D. Feng, and Z.W. Tian: *J. Electroanal. Chem.*, 1998, vol. 452, pp. 235–40.
31. E.A. Abdel-Aal, D. Dietrich, S. Steinhäuser, and B. Wielage: *Surf. Coat. Technol.*, 2008, vol. 202, pp. 5895–5900.
32. N. Dumelié, H. Benhayoune, C. Rousse-Bertrand, S. Bouthors, A. Perchet, L. Wortham, J. Douglade, D. Laurent-Maquin, and G. Balossier: *Thin Solid Films*, 2005, vol. 492, pp. 131–39.
33. I. Zhitomirsky: *Adv. Colloid Interface Sci.*, 2002, vol. 97, pp. 279–317.
34. N. Eliaz and M. Eliyahu: *J. Biomed. Mater. Res. A*, 2007, vol. 80, pp. 621–34.
35. R. Drevet, A. Viteaux, J.C. Maurin, and H. Benhayoune: *RSC Adv.*, 2013, vol. 3, pp. 11148–54.
36. S. Stanciu, A. Ursanu, L.C. Trinca, T.A. Elena, S. Carmen, C. Munteanu, N. Cimpoesu, D. Acatrinei, E.V. Sindilar, T. Stanciu, M. Fantanariu, and L. Topliceanu: *Environ. Eng. Manag. J.*, 2016, vol. 15, pp. 973–80.
37. R.I.M. Asri, W.S.W. Harun, M. Samykano, N.A.C. Lah, S.A.C. Ghani, F. Tarlochan, and M.R. Raza: *Mater. Sci. Eng. C*, 2017, vol. 77, pp. 1261–74.
38. U. Kamachimudali, T.M. Sridhar, and B. Raj: *Sadhana Acad. Proc. Eng. Sci.*, 2003, vol. 28, pp. 601–37.
39. R. Singh and N.B. Dahotre: *J. Mater. Sci. Mater. Med.*, 2007, vol. 18, pp. 725–51.